

Fine-scale recognition and use of mesoscale fronts by foraging Cape gannets in the Benguela upwelling region

Sabarros Philippe S.^{1,2,*}, Gremillet David^{3,4}, Demarcq Herve², Moseley Christina⁴, Pichegru Lorien⁴, Mullers Ralf H. E.³, Stenseth Nils C.^{1,5}, Machu Eric^{1,6,7}

¹ Univ Oslo, Dept Biol, Ctr Ecol & Evolutionary Synth, N-0316 Oslo, Norway.

² Inst Rech Dev, Ctr Rech Halieut Mediterranee & Trop, UMR EME 212, F-34203 Sete, France.

³ CNRS, Ctr Ecol Fonct & Evolut, F-34293 Montpellier, France.

⁴ Univ Cape Town, DST NRF Ctr Excellence, Percy Fitzpatrick Inst African Ornithol, ZA-7701 Rondebosch, South Africa.

⁵ Inst Marine Res, Flodevigen Marine Res Stn, N-4817 His, Norway.

⁶ Inst Rech Dev, Lab Phys Oceans, F-29280 Plouzane, France.

⁷ Ifremer, France

* Corresponding author : Philippe S. Sabarros, Tel.: +47 228 54 400; fax: +47 228 54 001 ; email address : p.s.sabarros@bio.uio.no

Abstract :

Oceanic structures such as mesoscale fronts may become hotspots of biological activity through concentration and enrichment processes. These fronts generally attract fish and may therefore be targeted by marine top-predators. In the southern Benguela upwelling system, such fronts might be used as environmental cues by foraging seabirds. In this study we analyzed high-frequency foraging tracks (GPS, 1 s sampling) of Cape gannets *Morus capensis* from two colonies located on the west and east coast of South Africa in relation to mesoscale fronts detected on daily high-resolution chlorophyll-a maps (MODIS, 1 km). We tested the association of (i) searching behavior and (ii) diving activity of foraging birds with mesoscale fronts. We found that Cape gannets shift from transiting to area-restricted search mode (ARS) at a distance from fronts ranging between 2 and 11 km (median is 6.7 km). This suggests that Cape gannets may be able to sense fronts (smell or vision) or other predators, and that such detection triggers an intensified investigation of their surroundings (i.e. ARS). Also we found that diving probability increases near fronts in 11 out of 20 tracks investigated (55%), suggesting that Cape gannets substantially use fronts for feeding; in the remaining cases (45%), birds may have used other cues for feeding including fishing vessels, particularly for gannets breeding on the west coast. We demonstrated in this study that oceanographic structures such as mesoscale fronts are important environmental cues used by a foraging seabird within the rich waters of an upwelling system. There is now need for further investigations on how Cape gannets actually detect these fronts.

Keywords : Seabird, Environmental cue, Behavioral shift, Area-restricted search, Feeding activity, Fractal landscape, Oceanographic fronts, *Morus capensis*, Southern Benguela, South Africa

55 INTRODUCTION

56

57 Oceanic circulation and light availability play a key role in structuring
58 ecosystems throughout the oceans. Oceanic circulation is crucial to supplying
59 nutrients to the layer that light penetrates, and thereby sustaining and shaping primary
60 productivity of marine food webs. Depending on the size, life span and diet of marine
61 species, primary production may constrain the distribution of marine species across
62 various spatiotemporal scales (Longhurst 1998). Hydrodynamic features – from larger
63 scales (100s km) to smaller scales (e.g. mesoscale, 1-2 km to 100-200 km) – are
64 known to drive the distribution and foraging patterns of top-predators because the
65 predictability of prey is higher in and around these structures (Weimerkirch 2007). It
66 has been well documented that large convergence zones (e.g. polar front) correspond
67 to foraging areas of marine birds and mammals (review by Bost et al. 2009). At
68 smaller scales, dynamic mesoscale structures such as eddies, vertically-structured
69 fronts and filaments are essential to the enrichment, concentration and retention of
70 nutrients and planktonic organisms in surface waters (*Bakun's triad*, cf Bakun 1996)
71 which attract and shape the aggregation patterns of plankton-eaters such as small
72 pelagic fish (Bakun 2006, Bertrand et al. 2008, Sabarros et al. 2009). Mesoscale
73 structures are considered as major attracting features for large predatory fish (Young
74 et al. 2001, Seki et al. 2002), marine mammals (Campagna et al. 2006, Cotté et al.
75 2007) and seabirds (Nel et al. 2001, Weimerskirch et al. 2004, 2005, Ainley et al.
76 2005, 2009, Hyrenbach et al. 2006).

77 How top-predators find these structures – notably fronts – still remains poorly
78 understood. Nevitt (2000, 2008) showed that a range of seabirds (procellariiforms)
79 track and capitalize on fronts across different scales using olfactory and visual cues.
80 Procellariiforms navigate at large scales by following odor compounds (e.g. dimethyl
81 sulfide) that are released by plankton organisms that accumulate at fronts. Once in the
82 visual range of fronts, procellariiforms may locate and dive onto fish patches. Only a
83 limited number of studies investigated the association between particular foraging
84 behavioral patterns in animal movements and environmental features. For example,
85 Trathan et al. (2008) showed that king penguins at South Georgia concentrate their
86 foraging effort to water masses with a particular temperature range, and Tew-Kai et
87 al. (2009) demonstrated that frigate birds feed at the edge of mesoscale eddies in the
88 Mozambique channel. There is a crucial need for such insight to improve our

89 understanding of the underlying mechanisms of seabird foraging behavior (Tremblay
90 et al. 2009).

91 Eastern boundary upwelling systems (EBUS) are subtropical coastal oceanic
92 regions where an important atmospheric forcing (i.e. winds) induces an offshore
93 transport of surface waters that are replaced by nutrient-rich waters from subsurface
94 layers (Capet et al. 2008). This newly upwelled water supports intense primary and
95 secondary production that sustains the world's highest fish biomass and fisheries
96 (Pauly & Christensen 1995, FAO 2001). In EBUS, mesoscale features such as eddies,
97 vertically-structured fronts, and filaments, are generated by the instability of
98 alongshore currents superimposed on the offshore Ekman transport of surface waters
99 (Capet et al. 2008) especially close to the shore (Pedlovsky 1978, Durski & Allen
100 2005). Local enrichment and concentration of nutrient in mesoscale features promotes
101 plankton production (Bakun 2006) and may thereby attract schools and clusters of
102 planktivorous fish (e.g. Ainley et al. 2005, Sabarros et al. 2009). Surface mesoscale
103 fronts associated to eddies, filaments and vertically-structured fronts are common in
104 the southern Benguela upwelling – one of the major EBUS – located off the coast of
105 South Africa and may well attract the most abundant planktivorous fish in that region
106 such as the sardine *Sardinops sagax* and the anchovy *Engraulis encrasicolus* (van der
107 Lingen et al. 2006). These pelagic fish constitute the main prey items of a medium-
108 ranging seabird: the Cape gannet *Morus capensis* that breeds at two colonies located
109 on the western and the eastern coasts of South Africa (Hockey et al. 2005). Cape
110 gannets forage within the productive waters of the Benguela upwelling system on the
111 continental shelf (Pichegru et al. 2007) and might therefore use fronts as
112 environmental cues when foraging. Foraging mechanisms and cues used by Cape
113 gannets are poorly known apart from the fact that Cape gannets sometimes scavenge
114 fishing boat discards on the west coast of South Africa (Grémillet et al. 2008).

115 The influence of mesoscale oceanic structures of only a few kilometers on the
116 distribution and foraging patterns of top predators has been little investigated due to
117 the difficulty of observing properly these patterns by satellites (e.g. Tew-Kai et al.
118 2009) or field measurements (e.g. van Franeker et al. 2002). Thanks to technological
119 advances in both satellite remote sensing (e.g. high-resolution chlorophyll-*a*
120 measurements) and seabird biotelemetry (e.g. high-frequency GPS) we are now able
121 to study foraging patterns of marine predators in relation to their environment at the
122 lower mesoscale (few kms). In the present study we use for the first time a

123 combination of high-precision individual GPS tracks (1 s sampling) of Cape gannets
124 and high-resolution daily maps of chlorophyll-*a* (1 km) provided by MODIS on which
125 we have identified mesoscale fronts (with edge detection algorithm). We assume here
126 that chlorophyll-*a* fronts are a proxy for the occurrence of seabirds' prey as shown in
127 various studies (e.g. [Ainley et al. 2005](#), [Bakun 2006](#), [Sabarros et al. 2009](#)). From GPS
128 tracks we have extracted the bird's searching behavior (i.e. area-restricted search
129 ARS) and feeding activity (i.e. dives). We use our datasets to test associations of (i)
130 searching behavior and (ii) diving activity with the presence and location of
131 mesoscale fronts in the Benguela upwelling system. We expect that the proximity of
132 fronts will induce intensified search patterns by Cape gannets and that feeding activity
133 will be concentrated around fronts.

134

135

136 MATERIAL AND METHODS

137

138 **Seabird tracks.**

139 Foraging movements of breeding Cape gannets were monitored at two South
140 African colonies during the reproductive season of 2009 (October-November). Adults
141 raising 2-6 week-old chicks were fitted with miniaturized high-precision GPS data-
142 loggers (TechnoSmart, Rome, Italy) that were sealed in heat-shrinkable tubing (120 x
143 55 x 30 mm; 45 g including waterproof housing). The unit weighted approximately
144 1.8% of the body mass of an adult gannet, which was below the 3% limit
145 recommended for deploying loggers on flying birds ([Phillips et al. 2003](#)). Loggers
146 were attached to the base of the tail (below the preen gland) on three central tail
147 feathers with waterproof Tesa tape. This attachment method did little damage to the
148 plumage and the tape could be removed entirely upon recapture ([Wilson et al. 1997](#)).
149 Handling lasted 4 to 10 min from capture to release. Nests were then monitored
150 regularly from 6h00 to 19h00 (South African standard time) until the bird returned.
151 The loggers recorded the position of the bird with an accuracy of 1-3 m, its speed, and
152 additional precision parameters (e.g. number of satellite signals received, dilution of
153 precision: DOP) every second. We selected the tracks that could be associated to
154 chlorophyll-*a* maps of decent quality (see "Chlorophyll-*a* data" part). We used a total
155 of 20 individual GPS tracks (no pseudo-replication) of which 9 were recorded on the
156 west coast at Malgas Island, Saldanha Bay (33°03'S, 17°55'E) and 11 on the east

157 coast at Bird Island, Mandela Bay (33°50'S, 26°17'E). Tracks are shown on Figure 1
158 and a summary of the track characteristics is provided in Table 1.

159

160 **Seabird foraging activity.**

161 *Area-restricted search (ARS)*. ARS describes an intense search activity performed
162 by a foraging animal that can be useful to study foraging activity and preferential
163 feeding grounds (Fauchald 2009, Tremblay et al. 2009). ARS behavior can be inferred
164 from animal movement data using the fractal landscape (FL) method (Tremblay et al.
165 2007). FL is based on the computation of a fractal measure: the fractal dimension D .
166 D measures the complexity and heterogeneity of a spatial or temporal object and
167 considers both time and space coverage. The principle of FL is to compute D along
168 the track inside a sliding time window as defined by Tremblay et al. (2007); here the
169 time window was approximately 1 h (Sabarros et al. in prep). The computation of D
170 was performed using the divider method, following Nams (1996). Straight pathways
171 are characterized by a D that is close to 1. D increases with track convolutions and
172 can readily detect intense foraging patterns characterized by frequent turns and
173 resultant tortuosity. In FL, the peaks of D found along the path represent the ARS
174 behavior (Tremblay et al. 2007, Sabarros et al. in prep).

175 *Feeding activity*. Cape gannets generally plunge dive from the air to catch prey
176 underwater, but occasionally perform surface-dives when sitting at the sea surface
177 (Ropert-Coudert et al. 2004). Dive durations generally average 2-5 s but dives > 5 s
178 may occur (Ropert-Coudert et al. 2004, Pichegru et al. 2007). When a GPS receiver is
179 submerged it stops collecting information sent by the satellite(s) since the signal is
180 lost. We used high-frequency tracks (1 s) to infer the location and duration of dives
181 from the interruptions in GPS signal. Dives were defined as interruptions > 1 s and <
182 30 s. Interruptions > 30 s are likely due to satellite signal reception problems or
183 receiver malfunctioning since Cape gannet maximum dive duration is 22 s (Ropert-
184 Coudert et al. 2004). Dive locations were assigned to the location fix preceding the
185 interruption of the signal. We rechecked every dive profiles (including speed and
186 signal reception) and found out that 95% of the interruptions in the signal >1 s and <
187 30 s corresponded to either plunge dives (see details in Supplementary Material S1) or
188 surface dives.

189

190 **Chlorophyll-*a* data.**

191 High-resolution satellite swaths (level 1 product, 1 km spatial resolution) of
192 chlorophyll-*a* from Moderate Resolution Imaging Spectroradiometer (MODIS)
193 satellite missions (Aqua and Terra) run by NASA (oceancolor.gsfc.nasa.gov) were
194 used to compile gridded daily maps at 1 km spatial resolution. Wavelengths of the
195 visible spectrum are used to monitor chlorophyll-*a*. Visible wavelengths are
196 sensitive to clouds, hence cloudy days lead to maps with poor data coverage. For the
197 purpose of our study, only cloud-free chlorophyll-*a* maps could be associated to bird
198 tracks.

199

200 **Mesoscale chlorophyll-*a* fronts.**

201 Fronts in upwelling areas were detected using an extension of the single-image
202 edge detection (SIED) algorithm of Canyula & Cornillon (1992) as described in Nieto
203 (2009). The basic idea of SIED method is to use overlapping windows to investigate
204 the statistical likelihood of an edge by detecting bimodality in histogram distribution
205 and checking for cohesiveness of the potential edge (Canyula & Cornillon 1992).
206 Nieto's method (2009) significantly improves the number and the length of boundaries
207 detected between water masses (compared to the original method) and allows the
208 detection of continuous fronts. The computation of SIED on high-resolution
209 chlorophyll-*a* maps allows the identification of surface oceanic features such as
210 mesoscale fronts. Fronts appear as curves and lines (see chlorophyll-*a* map with fronts
211 in Fig. 2).

212

213 **Fronts vs. seabird foraging behavior**

214 We chose to investigate the potential influence of fronts on Cape gannet
215 searching behavior and feeding activity by examining the proximity of foraging birds
216 to fronts. For each positional fix along the bird's pathway we calculated the distance
217 of the bird to all fronts and selected among them the distance of the bird to the nearest
218 front (*d*). Daily chlorophyll-*a* maps (with the position of fronts) were assigned to
219 tracks according to the date (generally spanning over one day, sometimes two days)
220 with a maximum lag of ± 1 day difference between the chlorophyll-*a* map and the
221 time of each positional fix considered (see Tab. 1). Fronts are dynamic structures and
222 the distance fronts can travel in 24 h may vary. Consecutive cloud-free maps of
223 chlorophyll-*a* were rarely available and we could not therefore evaluate front
224 displacement with precision. Fronts were however assumed to be relatively stable on

225 the short-term (e.g. 24 h) and their displacement to be negligible compared to the
226 distances covered by birds.

227 First, we investigated the influence of front distance on birds searching behavior.
228 Searching intensity was characterized by the fractal dimension D in the FL method
229 (Tremblay et al. 2007). For each track we generated figures with D calculated for each
230 positional fix on the Y-axis, and the corresponding distance to the nearest front d on
231 the X-axis (see Fig. 3, Supplementary Material S3). We designed an automated
232 algorithm to detect a potential behavioral shift on D relative to the distance d to the
233 nearest front: we systematically tested a range of 100 thresholds defined within the
234 range of d found in each track. Each threshold (d_{shift}) delimited two data subsets: the
235 first group corresponds to observations of D when $d \leq d_{shift}$, and the second group
236 when $d > d_{shift}$. We tested the difference in mean and variance between the two subsets
237 by using Student's t -tests and the F-tests (ANOVA) respectively. Because consecutive
238 calculations for D along the track are not independent from each other and because F-
239 test requires balanced data, we performed 1000 bootstraps of the method described
240 above by resampling in each empirical distribution a subset of size N that corresponds
241 to the smaller of the two subsets (Manly 2007). The position of the shift was chosen
242 as the distance threshold (d_{shift}) for which the difference in mean between the subsets
243 was the largest, and that verified that the respective means and variances were
244 significantly different (see example of this procedure in Supplementary Material S2).

245 Secondly, we tested the effect of the distance to the nearest front on diving
246 activity. We used a generalized linear model for binomial response (binomial
247 regression; logit link function) to explain the occurrence of diving events ($Dive$:
248 categorical response variable, $Dive = 1$ if dive occurs, $Dive = 0$ if not) relative to front
249 distance (d : explanatory variable). The probability to realize $Dive = 1$ was modeled as
250 a function of front distance: $\text{Pr}(z) = 1 / (1 + \exp(-z))$, where the probability to dive (Pr) is
251 a function of front distance (d in km) with z as the linear predictor $z = \alpha + \beta \oplus d$, α as
252 the intercept and β as the regression parameter on d . Because the number of
253 observations associated with dives (N_1) was often 100 times more than the number of
254 observations without dives (N_0) we used a bootstrap procedure to accommodate for
255 unbalanced observations of categorical data (Davison & Hinkley 1997, Manly 2007).
256 One bootstrap iteration consisted in resampling N_1 observations from the empirical
257 distribution of the non-associated-to-dives observations, and running the model

258 described above. Observations associated with dives were independent from each
259 other while observations non-associated with dives were originally correlated to each
260 other. By resampling N_1 from N_0 observations of $Dive = 0$ while $N_0 \gg N_1$, the
261 consecutive and dependent observations of $Dive = 0$ have less chance of appearing in
262 the same bootstrap subset, hence resolving the issue of non-independent data. We
263 performed 1000 bootstraps to obtain bootstrapped distributions for a , b , and the
264 associated p values. The probability and its bootstrapped 95% confidence interval
265 (drawn from 1000 simulations of $\Pr(Dive = 1 | d)$ with α and β in their respective
266 bootstrap distribution) were plotted as a function of d to illustrate the effect of the
267 latter on diving activity (see Fig. 5, see more in Supplementary Material S4).

268

269

270 RESULTS

271

272 *ARS behavior.*

273 The shift identification procedure (described and illustrated in Supplementary
274 Material S2) successfully identified in each track a threshold distance to the nearest
275 front (d_{shift}) that delimits two behavioral modes. Figure 3 illustrates this in track M2:
276 d_{shift} delimits a mode where D is higher and of greater variance near fronts ($d \leq d_{shift}$)
277 from a mode with a lesser D (close to 1) and with a reduced variance for locations that
278 are away from fronts ($d > d_{shift}$). This pattern was found in all investigated tracks (see
279 Supplementary Material S3), except tracks M7 and M8 that remained untested
280 because the computation of the FL method failed (technical issue we did not get a
281 chance to fix). Differences in mean and variance are significant (respectively t -test
282 and F-test with $p < 0.001$, Tab. 2). The threshold distance to the nearest front d_{shift}
283 ranges from 1.3 to 22 km with 6.7 km as the median (Fig. 4, Supplementary Material
284 S3).

285

286 *Feeding activity.*

287 Figure 2 shows a foraging trip performed by a Cape gannet from Malgas Island
288 (track M1). Dives located in the outermost part of the track occurred in the vicinity of
289 a front. The binomial regression parameter β (estimated by the bootstrap procedure)
290 that characterizes the effect of the distance to the nearest front d on diving is
291 presented in Table 2. The estimation for β significantly differs from 0 in 11 out of 20

292 tracks (55%, Tab. 2). This suggests that diving activity is significantly linked to the
293 distance of fronts in slightly more than half of the cases. This is illustrated in Figure 5
294 (example of track B1) by the negative relationship between the probability of diving
295 $\Pr(Dive = 1)$ and the distance to the nearest front d . Diving probability increases with
296 the proximity of fronts (Fig. 5 for track B1, see Supplementary Material S4 for the
297 other tracks). The probability that a dive occurs at the exact position of a front (i.e. at
298 $d = 0$) ranges from 0.56 to 0.87, with a median value of 0.69 (Tab. 3, Fig. 6). For
299 cases where the diving activity is not linked to fronts (45% of the tracks) this
300 probability ranges from 0.37 to 0.62 (median is 0.44, Tab. 2) and only varies
301 marginally with the distance of fronts (see Supplementary Material S4). When
302 comparing regions, we find that diving activity is significantly linked to fronts in 44%
303 of the tracks (4 out of 9 at Malgas Island) monitored on the west coast in contrast to
304 64% (7 out of 11 at Bird Island) on the east coast (Tab. 2).

305
306

307 DISCUSSION

308

309 Our study presents evidence that within the rich waters of the continental shelf of
310 the west and east coasts of the southern Benguela system Cape gannets track and use
311 oceanic structures such as mesoscale fronts. Here we provide new insights into the
312 mechanisms that link foraging patterns, i.e., searching (ARS) and feeding activity, to
313 the presence and location of mesoscale fronts. Searching behavior of Cape gannets
314 changes from transiting to ARS with the proximity of fronts and more than half the
315 birds feed substantially more near fronts.

316

317 **Detection of front triggers ARS**

318 Cape gannets exhibit a distinct behavioral shift when approaching fronts at a
319 median distance of 6.7 km. This behavioral shift delimits two modes: supposedly
320 active prey searching i.e. ARS ($D > 1$ with high variance), and transiting ($D \approx 1$ with
321 reduced variance). Near fronts, ARS mode is characterized by a higher D that
322 indicates that the pathway is convoluted and hence that the bird is actively
323 investigating the surroundings by making frequent turns. This ARS mode is also
324 characterized by a more variable D (i.e. high D but also low D parts) that suggests that
325 ARS is here a combination of convoluted and straight bouts. The transiting mode that

326 occurs away from fronts and that is characterized by straight movements likely
327 corresponds to commuting between colonies and feeding grounds for instance.

328 Perception of environmental cues is crucial to seabirds for acquiring reliable
329 information on their environment (Fauchald 2009). Fronts concentrate and enhance
330 biological activity and thus the predictability of finding prey is generally enhanced at
331 fronts regardless of the scale considered (Weimerskirch 2007, Bost et al. 2009). A
332 mesoscale chlorophyll-*a* front may correspond to the subduction between two water
333 masses that differ in chlorophyll-*a* concentration and hence in color (blue for low
334 chlorophyll-*a* concentrations and greenish for higher concentrations). Occasionally
335 there can be a local surface enhancement along the front (Capet et al. 2008). These
336 oceanographic structures can be detected by satellites (remote sensing, e.g. MODIS)
337 and probably by seabirds that fly over the oceans too. Here Cape gannets use
338 mesoscale fronts as environmental cues in the Benguela upwelling system. Tracking
339 these fronts and initiating ARS when detecting such structures may enable a medium-
340 ranging such as the Cape gannet to maximize prey encounters (see also Ainley et al.
341 2005).

342 Perception range is a critical aspect of sensory ecology since it is linked to
343 foraging success (Barraquand et al. 2009). Birds detecting fronts by sight would be
344 expected to initiate ARS at a relatively constant distance (liable to individual
345 variability) that would correspond to their visual range. This is clearly not the case in
346 our study since Cape gannets switch to ARS at distances ranging from 1.3 to 22 km.
347 Phytoplankton concentrated by fronts produces dimethyl sulfide (DMS) when grazed
348 by zooplankton. DMS can be sensed by a range of seabirds (procellariiforms) that use
349 this odor compound as a navigation cue (Nevitt 2000). Procellariiforms, for example,
350 use DMS to locate potential feeding zones at large scales, such as upwellings, sea
351 mounts and shelf breaks (Nevitt 2000, 2008). We argue that Cape gannets might also
352 be able to smell DMS emitted by phytoplankton, and hence use the odor landscape to
353 navigate towards favorable feeding areas and eventually trigger ARS. Depending on
354 wind speed and direction, DMS molecules may reach gannets at varying distances
355 from the location where they were emitted. This may explain why the distance of the
356 shift from transiting to ARS behavior varies by a factor of 17. Other predators'
357 behavior (e.g. congeners, other seabirds, subsurface predators) may inform a foraging
358 Cape gannet on the local environment and for example give indication on where to
359 concentrate its attention. Encountering by chance predators that seem to be heavily

360 searching for prey may drive a Cape gannet to initiate ARS. The predators used as
361 cues by Cape gannets may be located more or less close to a front or may not even be
362 associated to any front. This provides a possible explanation for the great variance
363 that characterizes the distance to fronts at which Cape gannets shift from transiting to
364 ARS. Finally, fronts are highly dynamic features and because the time lag between
365 the chlorophyll-*a* snapshots (daily maps) and the bird's positions reached 24 h in
366 some cases, this could be a source of error that would also explain the observed
367 variability in the behavioral shift distance.

368

369 **Fronts: selected feeding grounds**

370 Diving activity and by extension feeding activity of Cape gannets increases near
371 fronts in a substantial number of the GPS tracks investigated in this study (55%).
372 Fronts appear to be preferred feeding locations on these tracks, as the probability of
373 diving at fronts averages 0.7 (and is always higher than 0.56). As partly argued above,
374 Cape gannets may use a combination of olfactory and visual cues at smaller scales to
375 locate prey patches in the vicinity of fronts (comparably to procellariiforms, Nevitt
376 2000, 2008). The main prey of Cape gannets (sardine and anchovy) are planktivorous
377 fish (van der Lingen et al. 2006) and are therefore likely to be found in large
378 aggregations at/near fronts (e.g. Ainley et al. 2005, Bakun 2006, Sabarros et al. 2009).
379 Moreover, spotting prey in frontal zones may be facilitated by the presence of
380 subsurface predators (i.e. large predatory fish, pinnipeds, cetaceans or other seabirds)
381 that force fish schools towards the surface (Evans 1982, Le Corre & Jacquemet 2005).
382 At small scales again, fronts may be useful oceanic structures to capitalize on,
383 because once tracked by smell or other means, they allow prey detection by sight
384 from a closer distance.

385

386 **Use of other cues**

387 Diving activity was not increased near fronts compared to other locations in 45%
388 of the birds (N = 9/20) even though these birds exhibited a shift in searching behavior
389 that was related to fronts on larger scales. The probability of diving near fronts ranged
390 around 0.5 (0.37-0.62), indicating that diving was not linked to fronts. These birds
391 may have initiated ARS when detecting fronts but they probably used other cues for
392 feeding. There are a few possible explanations to that. Feeding activity may not be
393 associated with fronts in that case because these birds may have encountered patches

394 of prey in locations that are away from fronts while transiting for example
395 (Weimerskirch 2007, Sabarros et al. in prep). These Cape gannets may also have
396 found patches thanks to successful foraging congeners or other species (e.g. other
397 seabirds species, subsurface predators). Finally this may suggest that birds have
398 interacted with trawler boats like northern gannets in the UK (Votier et al. 2009).
399 Bottom trawlers in the southern Benguela generally fish along the continental break
400 shelf regardless of surface mesoscale fronts (see Fig. 1 in Grémillet et al. 2008).
401 Vessel monitoring systems (VMS) data from fishing boats would have been here
402 useful to test if Cape gannets do follow and interact with fishing boats (bottom
403 trawlers and purse-seiners).

404 The stocks of the preferred prey of Cape gannets (sardines and anchovies)
405 previously associated with the Western Cape province have shifted eastward in late
406 1990s towards the Eastern Cape province (Crawford et al. 2008). Following the
407 shortage of prey on the west coast, the population of Cape gannets in this region
408 decreased (Crawford et al. 2008). The eastward shift of prey has resulted in Cape
409 gannets of Malgas feeding extensively on fishery wastes (hake) discarded by trawlers
410 (Grémillet et al. 2008). This may explain the weaker association between feeding
411 activity and fronts on the west coast (44%) where gannets may follow fishing boats
412 compared to the east coast (64%) where birds seem not to feed on fishery wastes.

413

414 **Further directions**

415 Although the processes of concentration and enhancement of primary and
416 secondary productions at fronts are rather well known, the mechanisms that drive the
417 distribution and aggregation patterns of fish at fronts are still poorly understood
418 (except for very few studies e.g. Bertrand et al. 2008) and require particular attention,
419 including observational and modeling studies. Focusing on top-predators (a medium-
420 ranging seabird species here), we showed that foraging behaviors, i.e., searching and
421 feeding, are associated with external factors such as presence of mesoscale fronts.
422 One may imagine that such behaviors are tightly connected to underlying
423 physiological processes (involving energetic requirements, expenditure and
424 investment) so that the physiological state of a bird would drive his behavioral
425 response. The first step could be modeling the physiology of the bird using the
426 dynamic energy budget theory (DEB, Kooijman 2010). The second step could be
427 including this to a state-space model formulation in a Bayesian framework that would

428 manage the behavior aspect (e.g. Jonsen et al. 2005, Patterson et al. 2008) in the way
429 that the physiological states would induce changes in behavior.

430

431

432 ACKNOWLEDGEMENTS

433

434 The authors thank their respective affiliations listed above. Field studies on Cape
435 gannets were funded by the Percy FitzPatrick Institute of African Ornithology,
436 DST/NRF Center of Excellence at the University of Cape Town, South Africa, and by
437 the CEFÉ-CNRS in Montpellier, France. Permission to conduct research was obtained
438 from Cape Nature Conservation, West Coast National Parks, and South African
439 National Parks and we thank them for their extensive logistics support. Philippe S.
440 Sabarros thanks Marie Curie actions under FP6 (MEST-CT-2005-020932) through
441 the CEES-MCO training site, and Norwegian Research Council (NFR-179569/V70).
442 Eric Machu thanks the MICO project (NFR-ES427093). We are grateful to Tristan
443 Rouyer for guidance on statistical analysis.

444

445

446 REFERENCES

447

- 448 Ainley DG, Dugger KD, Ford RG, Pierce SD, Reese DC, Brodeur RD, Tynan CT,
449 Barth JA (2009) Association of predators and prey at frontal features in the
450 California Current: competition, facilitation and co-occurrence. *Marine Ecology*
451 *Progress Series* 389:271-294
- 452 Ainley DG, Spear LB, Tynan CT, Barth JA, Pierce SD, Glenn Ford R, Cowles TJ
453 (2005) Physical and biological variables affecting seabird distributions during the
454 upwelling season of the northern California Current. *Deep-Sea Research II*
455 52:123-143
- 456 Bakun A (2006) Fronts and eddies as key structures in the habitat of marine fish
457 larvae: opportunity, adaptive response and competitive advantage. *Scientia Marina*
458 70S2:105-122
- 459 Bakun A (1996) *Patterns in the ocean: ocean processes and marine population*
460 *dynamics*. University of California Sea Grant, San Diego, California, USA, in
461 cooperation with Centro de Investigaciones Biológicas de Noroeste, La Paz, Baja

462 California Sur, Mexico. 323 pp.

463 Barraquand F, Inchausti P, Bretagnolle V (2009) Cognitive abilities of a central place
464 forager interact with prey spatial aggregation in their effect on intake rate.
465 *Animal Behaviour* 78:505-214

466 Bertrand A, Gerlotto F, Bertrand S, Gutiérrez M, Alza L, Chipollini A, Díaz E,
467 Espinoza P, Ledesma J, Quesquén R, Peraltilla S, Chavez F (2008) Schooling
468 behaviour and environmental forcing in relation to anchoveta distribution: An
469 analysis across multiple spatial scales. *Progress in Oceanography* 79:164-277

470 Bost CA, Cotté C, Bailleul F, Cherel Y, Charassin J-B, Guinet C, Ainley DG,
471 Weimerskirch H (2009) The importance of oceanographic fronts to marine birds
472 and mammals of the southern oceans. *Journal of Marine Systems* 78:363-376

473 Canyula JF, Cornillon (1992) Edge detection algorithm for SST images. *Journal of*
474 *Atmospheric and Oceanic Technology* 9:67-80

475 Campagna C, Piola AR, Rosa Marin M, Lewis M, Fernández T (2006) Southern
476 elephant seal trajectories, fronts and eddies in the Brazil/Malvinas Confluence.
477 *Deep-Sea Research I* 53:1907-1924

478 Capet X, Colas F, Penven P, Marchesiello P, McWilliams J (2008) Eddies in eastern
479 boundary subtropical upwelling systems. In: *Eddy-resolving ocean modeling*,
480 Hecht M and Hasumi H eds. AGU Monograph, vol. 177, Washington, DC. p 350

481 Cotté C, Park YH, Guinet C, Bost CA (2007) Movements of foraging king penguins
482 through marine mesoscale eddies. *Proceedings of the Royal Society B* 274:2385-
483 2391

484 Crawford RJM, Sabarros PS, Fairweather T, Underhill LG, Wolfaardt AC (2008)
485 Implications for seabirds of a long-term change in the distribution of sardine: a
486 South African experience. *African Journal of Marine Science* 30(1):177-184

487 Davison AC, Hinkley DV (1997) *Bootstrap methods and their application*.
488 Cambridge University Press

489 Durski SM, Allen JS (2005) Finite-amplitude evolution of instabilities associated with
490 the coastal upwelling front. *Journal of Physical Oceanography* 35:1606-1628

491 Evans PGH (1982) Associations between seabirds and cetaceans: a review. *Mammal*
492 *Review* 12(4):187-206

493 Fauchald P (2009) Spatial interaction between seabirds and prey: review and
494 synthesis. *Marine Ecology Progress Series* 391:139-151

495 van Franeker J, van den Brink N, Bathmann UV, Pollard RT, de Baar HJW, Wolff WJ

496 (2002) Responses of seabirds, in particular prions (*Pachyptila* sp.), to small-scale
497 processes in the Antarctic Polar Front. Deep-Sea Research II 49:3931-3950
498 Grémillet D, Pichegru L, Kuntz G, Woakes AG, Wilkinson S, Crawford RJM, Ryan
499 PG (2008) A junk-food hypothesis for gannets feeding on fishery waste.
500 Proceedings of the Royal Society B 275:1149-1156
501 Hockey P, Dean WRJ, Ryan PG (2005) *Roberts Birds of Southern Africa*. John
502 Voelker Bird Book Fund
503 Hyrenbach KD, Veit RR, Weimerskirch H, Hunt GL (2006) Seabird associations with
504 mesoscale eddies: the subtropical Indian Ocean. Marine Ecology Progress Series
505 324:271-279
506 Jonsen ID, Mills_Flemming J, Myers RA (2005) Robust state-space modeling of
507 animal movement data. Ecology 86(11):2874-2880
508 Kooijman SALM (2010) *Dynamic energy budget theory for metabolic organisation*.
509 Cambridge University Press
510 Le Corre M, Jaquemet S (2005) Assessment of seabird community of the
511 Mozambique Channel and its potential use as indicator of tuna abundance.
512 Estuarine, Coastal and Shelf Science 63:421-428
513 van der Lingen C, Hutchings L, Field JG (2006) Comparative trophodynamics of
514 anchovy *Engraulis encrasicolus* and sardine *Sardinops sagax* in the southern
515 Benguela: are species alternations between small pelagic fish trophodynamically
516 mediated? African Journal of Marine Science 28(34):465-477
517 Longhurst AR (1998) *Ecological geography of the sea*. Academic Press
518 Manly BFJ (2006) *Randomization, bootstrap and Monte Carlo methods in biology*
519 Chapman & Hall/CRC
520 Nams VO (1996) The VFractal: a new estimator for fractal dimension of animal
521 movement paths. Landscape Ecology 11(5):289-297
522 Nel DC, Lutjeharms JRE, Pakhomov EA, Ansorge IJ, Ryan PG, Klages NTW (2001)
523 Exploitation of mesoscale oceanographic features by grey-headed albatross
524 *Thalassarche chrysostoma* in the southern Indian Ocean. Marine Ecology
525 Progress Series 217:15-26
526 Nevitt GA (2008) Sensory ecology on the high seas: the odor world of the
527 procellariiform seabirds. Journal of Experimental Biology 211:1706-1713
528 Nevitt GA (2000) Olfactory foraging by Antarctic procellariiform seabirds: Life at
529 high Reynolds numbers. Biology Bulletin 198:245-253

530 Nieto K (2009) *Variabilidad oceánica de mesoescala en los ecosistemas de*
531 *afloresamiento de Chile y Canarias: una comparación a partir de datos satelitales.*
532 PhD thesis, University of Salamanca

533 Patterson TA, Thomas L, Wilcox C, Ovaskainen O, Matthiopoulos J (2008) Space-
534 state models of individual animal movement. *Trends in Ecology and Evolution*
535 23(2):87-94

536 Pauly D, Christensen V (1995) Primary production required to sustain global
537 fisheries. *Nature* 374:255-257

538 Pedlosky J (1978) A nonlinear model of the onset of upwelling. *Journal of Physical*
539 *Oceanography* 8:178-187

540 Phillips RA, Xavier JC, Croxall JP (2003) Effects of satellite transmitters on
541 albatrosses and petrels. *The Auk* 120(4):1082-1090

542 Pichegru L, Ryan PG, der Lingen CDV, Coetzee J, Ropert-Coudert Y, Grémillet D
543 (2007) Foraging behaviour and energetics of Cape gannets *Morus capensis*
544 feeding on live prey and fishery discards in the Benguela upwelling system.
545 *Marine Ecology Progress Series* 350:127-136

546 Ropert-Coudert Y, Grémillet D, Ryan P, Kato A, Naito Y, Le Maho Y (2004)
547 Between air and water: the plunge dive of the Cape Gannet *Morus capensis*. *Ibis*
548 146:281-290

549 Sabarros PS, Grémillet D, Stenseth NC, Ryan PG, Machu E (in prep) A critical
550 assessment of area-restricted search methods to identify feeding activity in
551 seabird foraging movements.

552 Sabarros PS, Ménard F, Lévénez J-J, Tew-Kai E, TERNON J-F (2009) Mesoscale eddies
553 influence distribution and aggregation patterns of micronekton in the
554 Mozambique Channel. *Marine Ecology Progress Series* 395:101-107

555 Seki MP, Polovina JJ, Kobayashi DR, Bidigare RR, Mitchum GT (2002) An
556 oceanographic characterization of swordfish (*Xiphias gladius*) longline fishing
557 grounds in the springtime subtropical North Pacific. *Fisheries Oceanography*
558 11:5:251-266

559 Tew-Kai E, Rossi V, Sudre J, Weimerskirch H, Lopez C, Hernandez-Garcia E,
560 Marsac F, Garçon V (2009) Top marine predators track Lagrangian coherent
561 structures. *Proceedings of the National Academy of Sciences USA* 106(20):8245-
562 8250

563 Trathan PN, Bishop C, Maclean G, Brown P, Fleming A, Collins MA (2008) Linear

564 tracks and restricted temperature ranges characterise penguin foraging pathways.
565 Marine Ecology Progress Series 370:285-294

566 Tremblay Y, Bertrand S, Henry RW, Kappes MA, Costa DP, Schaffer SA (2009) A
567 review of analytical approaches to investigate seabird-environment interactions.
568 Marine Ecology Progress Series 391:153-163

569 Tremblay Y, Roberts AJ, Costa DP (2007) Fractal landscape method: an alternative
570 approach to measuring area-restricted searching behavior. Journal of
571 Experimental Biology 210:935-945

572 Votier SC, Bearhop S, Witt MJ, Inger R, Thompson D, Newton J (2010) Individual
573 responses of seabirds to commercial fisheries revealed using GPS tracking, stable
574 isotopes and vessel monitoring systems. Journal of Applied Ecology 47:487-497

575 Weimerskirch H (2007) Are seabirds foraging for unpredictable resources? Deep-Sea
576 Research II 54:211-223

577 Weimerskirch H, Le Corre M, Jaquemet S, Potier M, Marsac F (2004) Foraging
578 strategy of a top predator in tropical waters: great frigatebirds in the Mozambique
579 Channel. Marine Ecology Progress Series 275:297-308

580 Weimerskirch H, Le Corre M, Ropert-Coudert Y, Kato A, Marsac F (2005) The three-
581 dimensional flight of red-footed boobies: adaptations to foraging in a tropical
582 environment?. Proceedings of Royal Society London B 272(1558):53-61

583 Wilson RP, Putz K, Peters G, Culik B, Scolaro JA, Charrassin J-B, Ropert-Coudert Y
584 (1997) Long-term attachment of transmitting and recording devices to penguins
585 and other seabirds. Wildlife Society Bulletin 25:101-106

586 Young JW, Bradford R, Lamb TD, Clementson LA, Kloser R, Galea H (2001)
587 Yellowfin tuna (*Thunnus albacares*) aggregations along the shelf break off south-
588 eastern Australia: links between inshore and offshore processes. Marine and
589 Freshwater Research 52:463-474

590
591

592 FIGURE AND TABLE CAPTIONS

593

594 Figure 1. Cape gannet tracks (N = 20) recorded in October-November 2009 on the
595 western and eastern coasts of South Africa. Figure 2. Cape gannet track (M1) recorded
596 on 24-25/10/2009 (red line) on the west coast of South Africa superimposed onto the
597 corresponding chlorophyll-*a* concentrations map (1 km spatial resolution; mg m⁻³, see

598 color scale) with front locations (dark blue lines). Dots indicates feeding spots.
599 Figure 3. Behavioral shift in track M2 (24-25/10/09, Malgas Island). Fractal
600 dimension D that was computed along the track is given as a function of distance to
601 front d ($N = 90000$ observations). Vertical dotted line indicates the shift at $d = d_{shift}$.
602 Horizontal solid lines are the means in the subsets $\leq d_{shift}$ and $> d_{shift}$ and horizontal
603 dashed lines represent the lower and upper quantiles (95%).

604

605 Figure 4. Behavioral shift distance to the nearest front (d_{shift}). $N = 18$ tracks. Median is
606 6.7 km.

607

608 Figure 5. Probability of diving as a function of the distance to the nearest front in
609 track B1 (21-22/11/09, Bird Island). Solid line represents the mean effect and dashed
610 lines represent 95% confidence interval. The density of observations of diving activity
611 is given for $Dive = 1$ and $Dive = 0$ along the X-axis (grey shading).

612

613 Figure 6. Diving probability at front ($d = 0$) for tracks associated with fronts and those
614 with no association. Horizontal dotted line marks a probability of 0.5. In tracks
615 associated with fronts the median is 0.7, and 0.46 for those not associated with fronts.

616

617 Table 1. Cape gannet tracks, foraging parameters and corresponding date of the
618 chlorophyll- a maps.

619

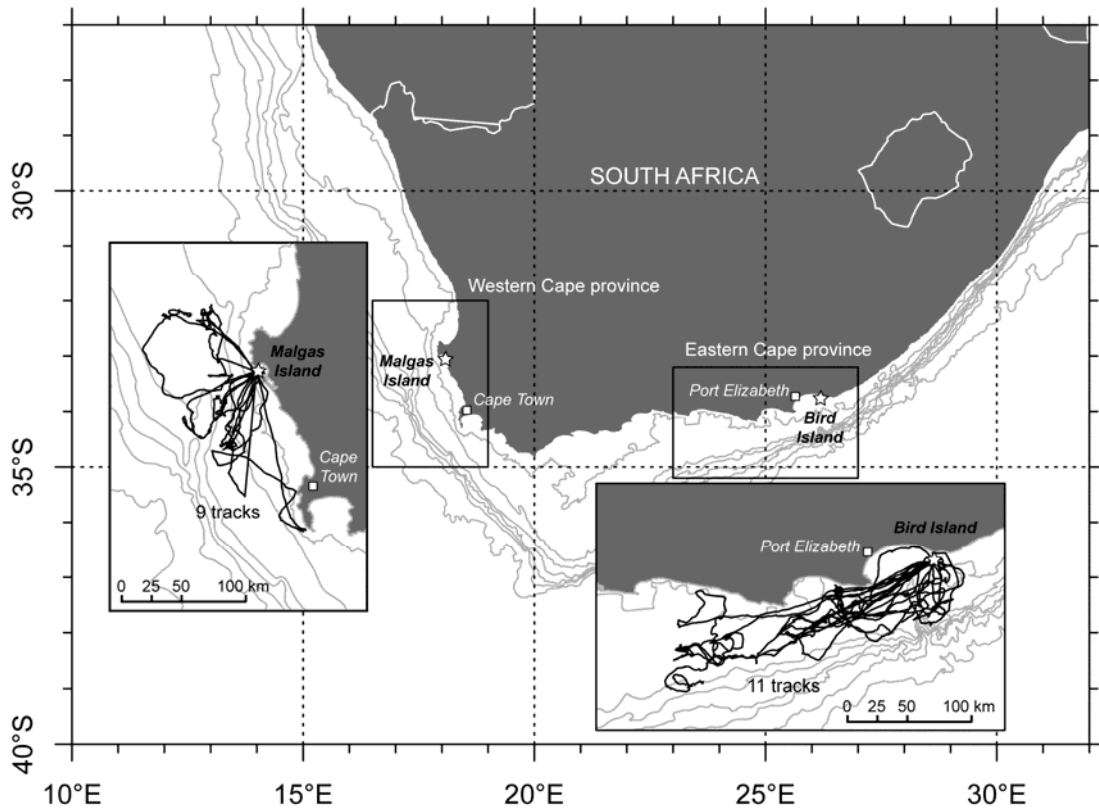
620 Table 2. Influence of fronts on ARS and diving activity. “*” indicates that the 95%
621 bootstrapped confidence interval of β does not overlap with 0 and that β is therefore
622 significantly different from 0. FL computation failed for M7 and M9 (indicated by “-
623 ”).

1 FIGURES

2 Fine-scale recognition and use of mesoscale fronts by foraging Cape gannets in the
3 Benguela upwelling region – Sabarros *et al.*

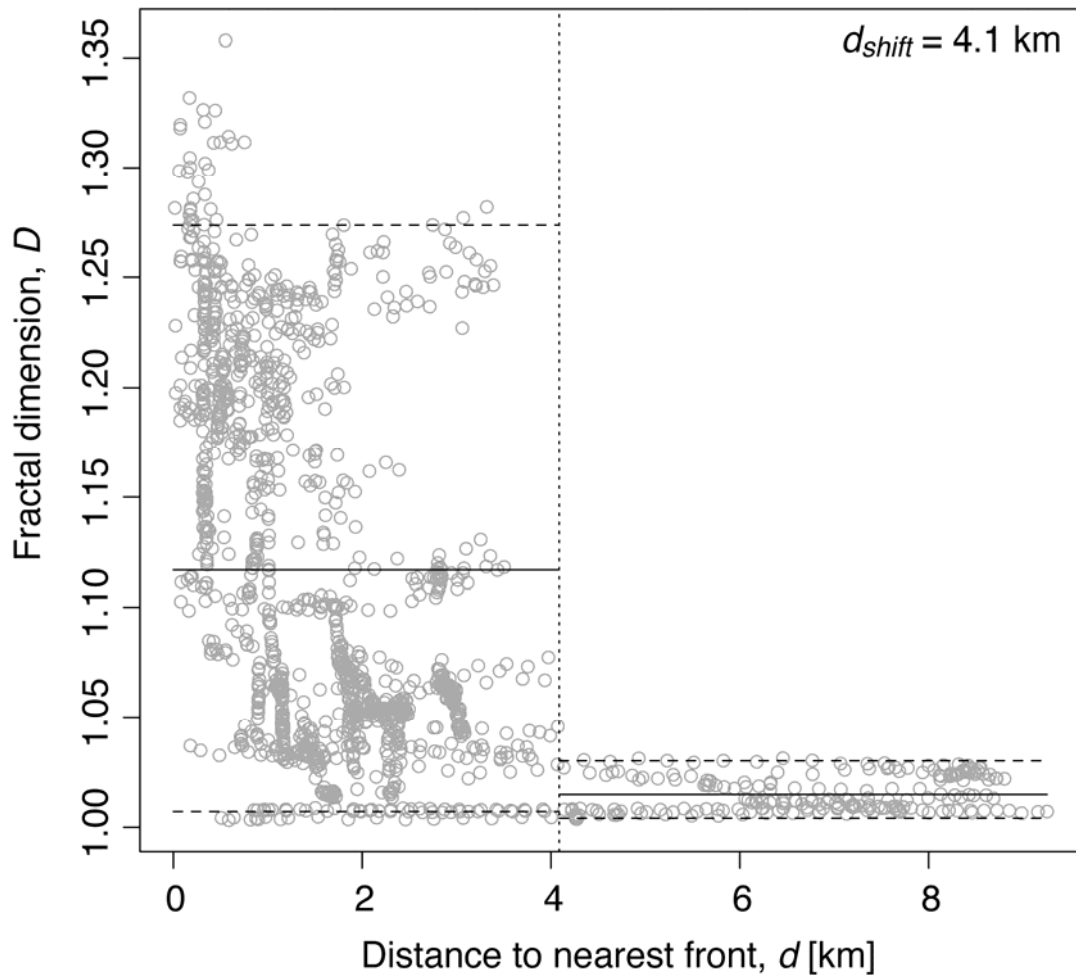
4

5



6 Figure 1. Cape gannet tracks (N = 20) recorded in October-November 2009 on the
7 western and eastern coasts of South Africa.

Track M2



12

13 Figure 3. Behavioral shift in track M2 (24-25/10/09, Malgas Island). Fractal
14 dimension D (= searching intensity) was computed along the track and is given as a
15 function of distance to front d ($N = 90000$ observations). Vertical dotted line indicates
16 the shift at $d = d_{shift}$. Horizontal solid lines are the means in the subsets $\leq d_{shift}$ and $>$
17 d_{shift} and horizontal dashed lines represent the lower and upper quantiles (95%).



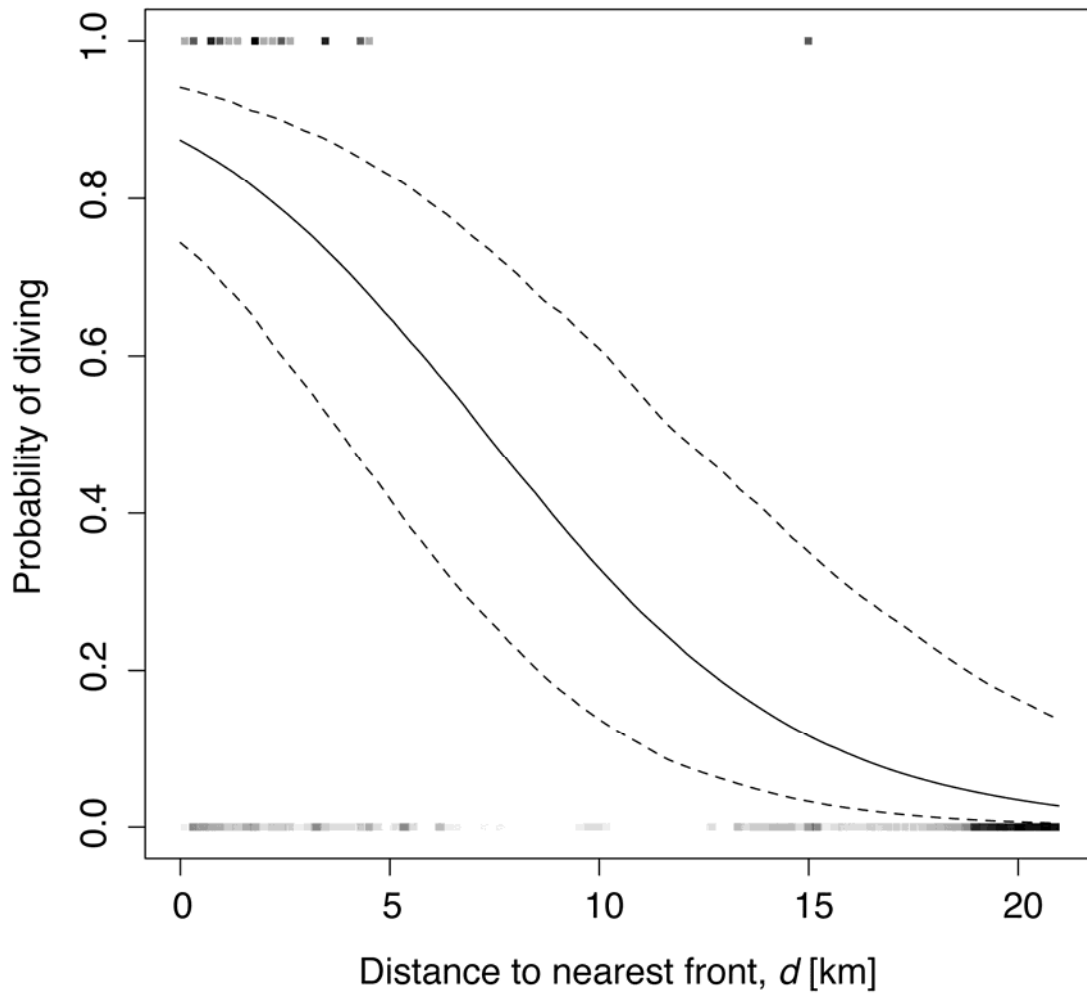
18

19 Figure 4. Behavioral shift distance to the nearest front (d_{shift}). N = 18 tracks. Median is

20 6.7 km.

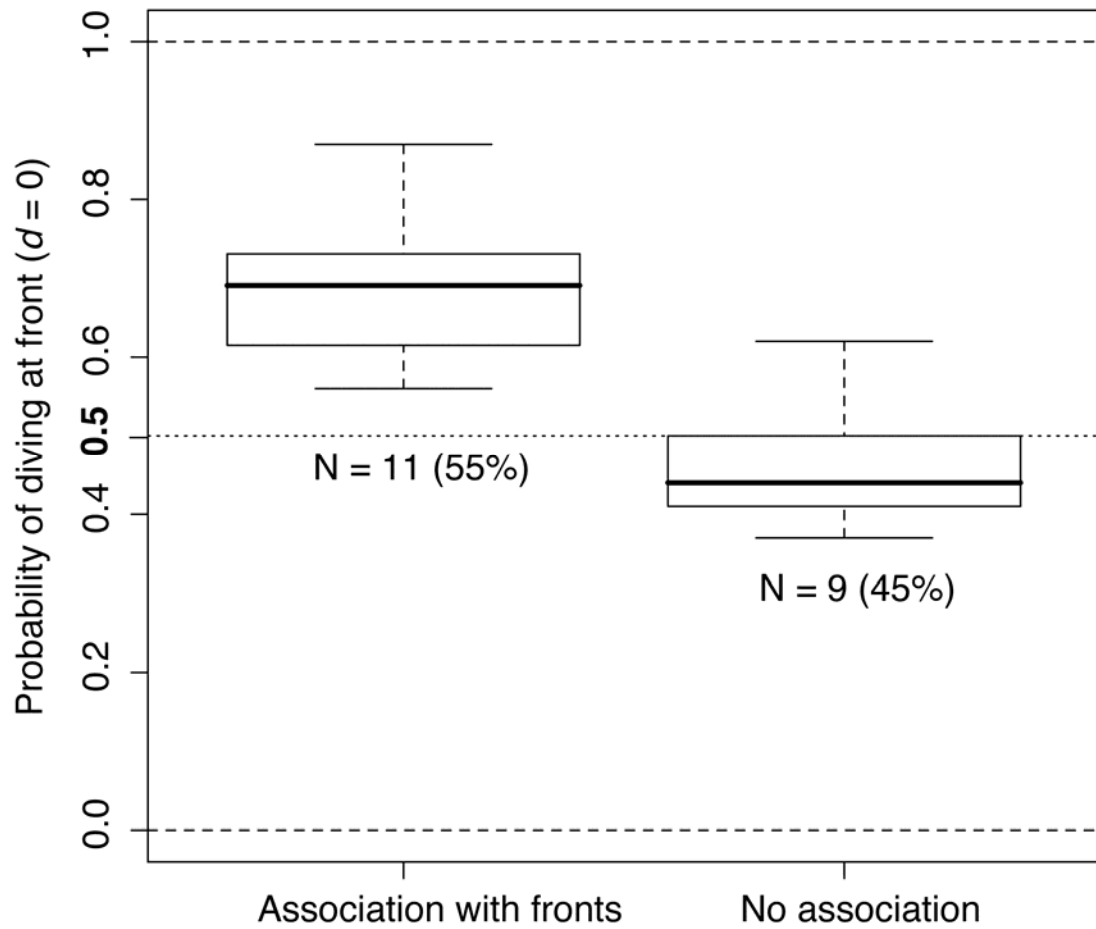
21

Track B1



22

23 Figure 5. Probability of diving as a function of the distance to the nearest front in
24 track B1 (21-22/11/09, Bird Island). Solid line represents the mean effect and dashed
25 lines represent 95% confidence interval. The density of observations of diving activity
26 is given for $Dive = 1$ and $Dive = 0$ along the X-axis (grey shading).



27

28 Figure 6. Diving probability at front ($d = 0$) for tracks associated with fronts and those

29 with no association. Horizontal dotted line marks a probability of 0.5. In tracks

30 associated with fronts the median is 0.7, and 0.46 for those not associated with fronts.

31 TABLES

32

33 Table 1. Cape gannet tracks, foraging parameters and corresponding date of the

34 chlorophyll-*a* maps.

| Track ID | Track name | Colony | Date | Trip duration [h] | Path length [km] | N dives | chl-<i>a</i> map(s) |
|-----------------|-------------------|---------------|-------------|--------------------------|-------------------------|----------------|----------------------------|
| M1 | T0A_24OC | Malgas | 24-25/10/09 | 25.2 | 313 | 68 | 25/10/09 |
| M2 | T0B_24OC | Malgas | 24-25/10/09 | 8.8 | 280 | 36 | 25/10/09 |
| M3 | T0C_25OC | Malgas | 25-26/10/09 | 9.54 | 278 | 69 | 25/10/09 |
| M4 | T14_25OC | Malgas | 25-26/10/09 | 15.84 | 297 | 59 | 25/10/09 |
| M5 | T08_14NV | Malgas | 14-15/11/09 | 21.6 | 363 | 26 | 15/11/09 |
| M6 | T0E_20NV | Malgas | 20-21/11/09 | 21.93 | 433 | 88 | 21/11/09 |
| M7 | T0C_21NV | Malgas | 20-21/11/09 | 21.8 | 357 | 48 | 21/11/09 |
| M8 | T0C_22NV | Malgas | 22-23/11/09 | 19.86 | 309 | 58 | 22-23/11/09 |
| M9 | T0E_22NV | Malgas | 22-23/11/09 | 22.85 | 532 | 61 | 23/11/09 |
| B1 | BI-13-96_21-11-09 | Bird | 21-22/11/09 | 15.31 | 228 | 27 | 22/11/09 |
| B2 | BI-32-10_23-11-09 | Bird | 23-24/11/09 | 21.22 | 395 | 77 | 23/11/09 |
| B3 | BI-33-16_23-11-09 | Bird | 23-24/11/09 | 19.67 | 403 | 58 | 23/11/09 |
| B4 | BI-48-78_27-11-09 | Bird | 27-28/11/09 | 10.09 | 305 | 28 | 28/11/09 |
| B5 | BI-49-12_27-11-09 | Bird | 27-28/11/09 | 21.21 | 438 | 54 | 28/11/09 |
| B6 | BI-50-96_27-11-09 | Bird | 27-28/11/09 | 22.8 | 517 | 28 | 28/11/09 |
| B7 | BI-51-10_27-11-09 | Bird | 27-28/11/09 | 26.38 | 607 | 151 | 28/11/09 |
| B8 | BI-52-13_28-11-09 | Bird | 28-29/11/09 | 24.85 | 737 | 49 | 28/11/09 |
| B9 | BI-53-78_28-11-09 | Bird | 28-29/11/09 | 18.74 | 481 | 22 | 28/11/09 |
| B10 | BI-54-11_28-11-09 | Bird | 28-29/11/09 | 28.12 | 923 | 105 | 28/11/09 |
| B11 | BI-56-14_28-11-09 | Bird | 28-29/11/09 | 33.01 | 703 | 93 | 28/11/09 |

35 Table 2. Influence of fronts on ARS and diving activity. “*” indicates that the 95% bootstrapped confidence interval of β does not overlap with 0
 36 and that β is therefore significantly different of 0. FL computation failed for M7 and M9 (indicated by “-”).

| Track ID | d_{shift} [km] | ARS activity | | | | | Diving activity | | | | |
|----------|------------------|---------------------------|------------------------|------------|------------|------------|------------------|---------|-----------------|-------------------------|------------------|
| | | mean $D/d \leq d_{shift}$ | mean $D/d > d_{shift}$ | ΔD | p T-test | p F-test | Linked to fronts | β | IC 95% | Pr(Dive = 1 $d = 0$) | Linked to fronts |
| M1 | 3.1 | 1.101 | 1.029 | -0.072 | < 0.001 | < 0.001 | Yes | -0.35 | [-0.53, -0.19]* | 0.76 | Yes |
| M2 | 4.1 | 1.117 | 1.015 | -0.102 | < 0.001 | < 0.001 | Yes | -0.17 | [-0.33, 0.02] | 0.59 | No |
| M3 | 4.7 | 1.076 | 1.012 | -0.064 | < 0.001 | < 0.001 | Yes | -0.01 | [-0.12, 0.09] | 0.50 | No |
| M4 | 3.3 | 1.048 | 1.020 | -0.028 | < 0.001 | < 0.001 | Yes | 0.12 | [-0.01, 0.28] | 0.37 | No |
| M5 | 6.9 | 1.034 | 1.008 | -0.026 | < 0.001 | < 0.001 | Yes | 0.10 | [-0.18, 0.46] | 0.42 | No |
| M6 | 8.3 | 1.033 | 1.011 | -0.022 | < 0.001 | < 0.001 | Yes | -0.05 | [-0.09, -0.01]* | 0.56 | Yes |
| M7 | - | - | - | - | - | - | - | -0.11 | [-0.27, 0.02] | 0.62 | No |
| M8 | 4.9 | 1.071 | 1.018 | -0.053 | < 0.001 | < 0.001 | Yes | -0.24 | [-0.37, -0.11]* | 0.72 | Yes |
| M9 | - | - | - | - | - | - | - | -0.19 | [-0.28, -0.12]* | 0.64 | Yes |
| B1 | 2.1 | 1.048 | 1.008 | -0.040 | < 0.001 | < 0.001 | Yes | -0.26 | [-0.34, -0.20]* | 0.87 | Yes |
| B2 | 8.3 | 1.049 | 1.005 | -0.044 | < 0.001 | < 0.001 | Yes | -0.08 | [-0.14, -0.01]* | 0.56 | Yes |
| B3 | 12 | 1.020 | 1.004 | -0.015 | < 0.001 | < 0.001 | Yes | -0.23 | [-0.35, -0.12]* | 0.65 | Yes |
| B4 | 6.4 | 1.039 | 1.010 | -0.029 | < 0.001 | < 0.001 | Yes | -0.10 | [-0.16, 0.04]* | 0.68 | Yes |
| B5 | 19 | 1.012 | 1.005 | -0.007 | < 0.001 | < 0.001 | Yes | -0.11 | [-0.19, -0.04]* | 0.70 | Yes |
| B6 | 22 | 1.016 | 1.005 | -0.011 | < 0.001 | < 0.001 | Yes | 0.04 | [-0.04, 0.14] | 0.40 | No |
| B7 | 9.2 | 1.025 | 1.005 | -0.020 | < 0.001 | < 0.001 | Yes | 0.09 | [-0.01, 0.23] | 0.41 | No |
| B8 | 1.3 | 1.069 | 1.014 | -0.055 | < 0.001 | < 0.001 | Yes | -0.38 | [-0.54, -0.24]* | 0.74 | Yes |
| B9 | 17 | 1.010 | 1.006 | -0.004 | < 0.05 | < 0.05 | Yes | 0.03 | [-0.06, 0.12] | 0.44 | No |
| B10 | 4.7 | 1.053 | 1.011 | -0.042 | < 0.001 | < 0.001 | Yes | -0.09 | [-0.13, -0.05]* | 0.59 | Yes |
| B11 | 15 | 1.021 | 1.001 | -0.020 | < 0.001 | < 0.001 | Yes | 0.02 | [-0.05, 0.11] | 0.48 | No |

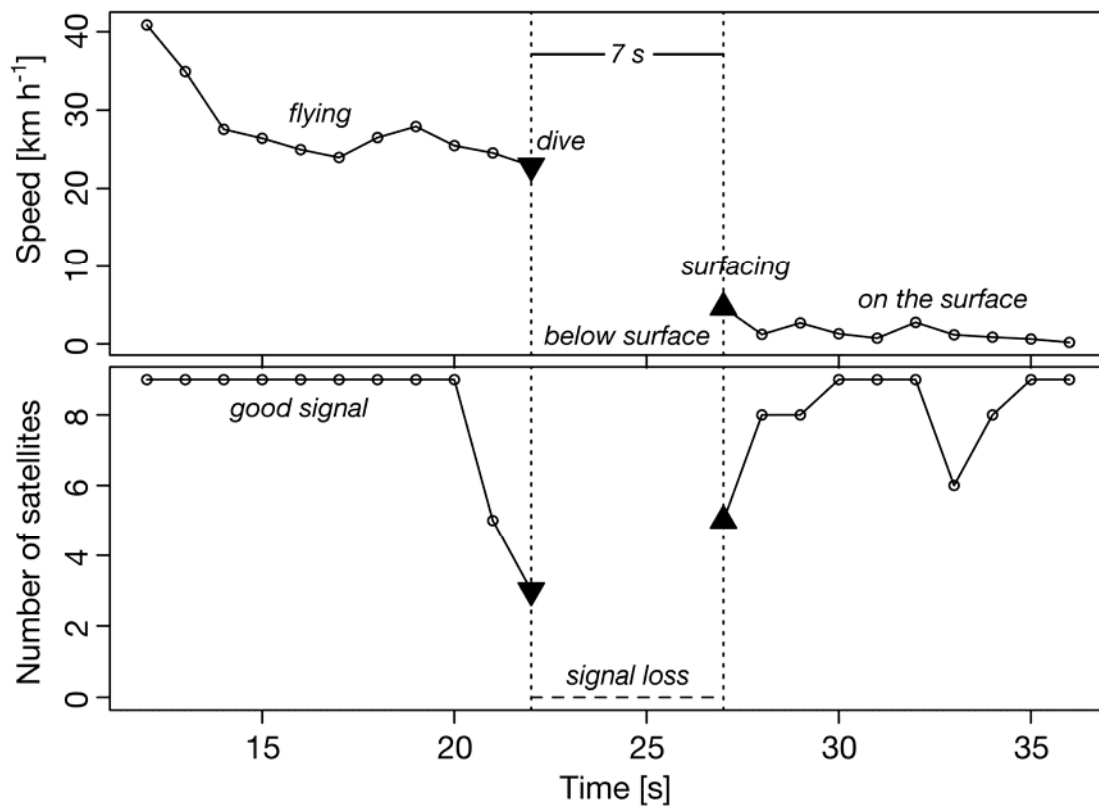
1 SUPPLEMENTARY MATERIAL

2 Fine-scale recognition and use of mesoscale fronts by foraging Cape gannets in the
3 Benguela upwelling region – Sabarros *et al.*

4

5 **Section 1. Dive profile and identification**

6



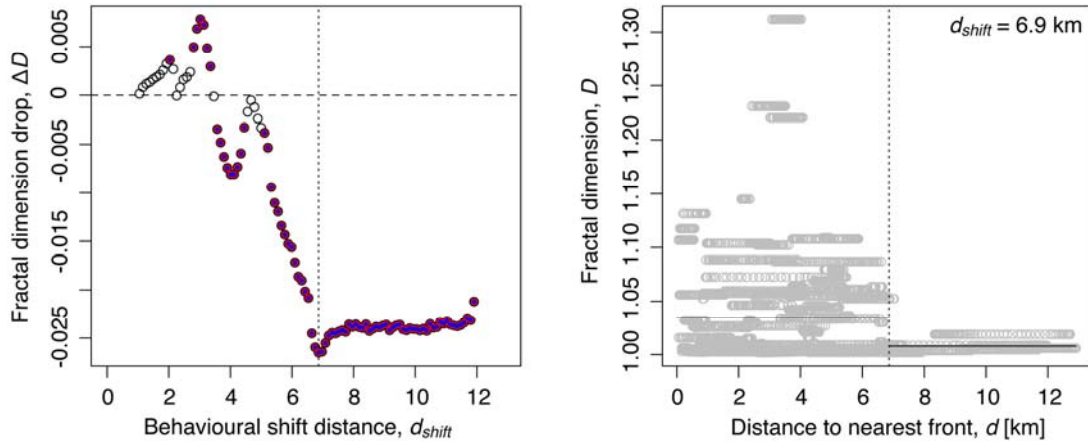
7

8 Figure S1. Plunge dive of a Cape gannet. (a) Speed and (b) number of satellite signals
9 received are shown to illustrate the signal interruption when the bird dives. The
10 example is taken from track BI-8-78_20-11-09 (14th dive).

11 Section 2. Behavior shift identification

12

Track M5



13

14 Figure S2. Behavior shift identification method. (a) Drop in fractal dimension D

15 between the subset $\leq d_{shift}$ and $> d_{shift}$ as a function of the distance threshold (d_{shift}).

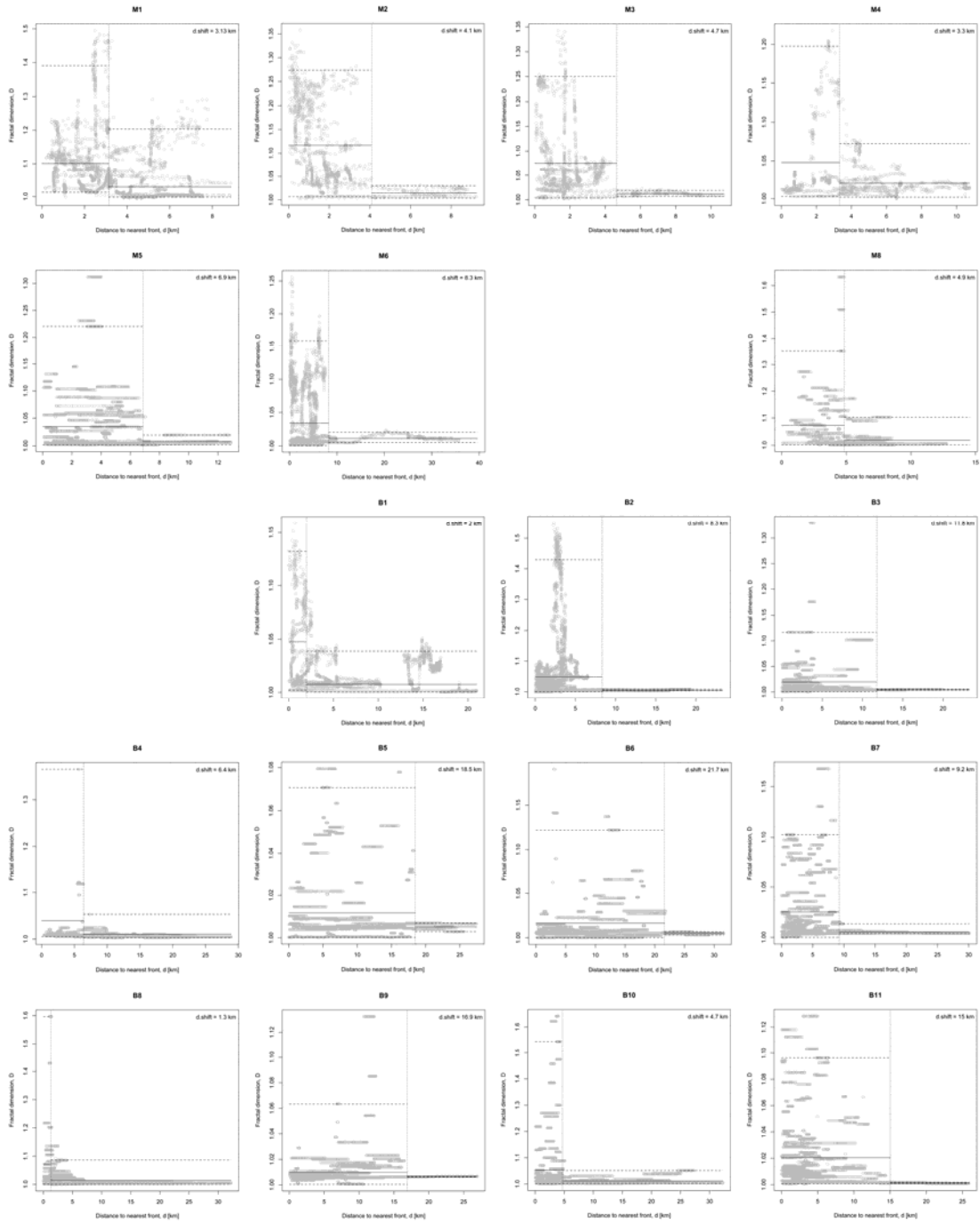
16 The blue filling and red circling of the dots indicate that, respectively, the t -test

17 (difference in mean) and the F -test (variance difference) comparing the two subsets

18 delimited by d_{shift} are significant. (b) Fractal dimension D as a function of d showing

19 the behavior shift for the selected d_{shift} .

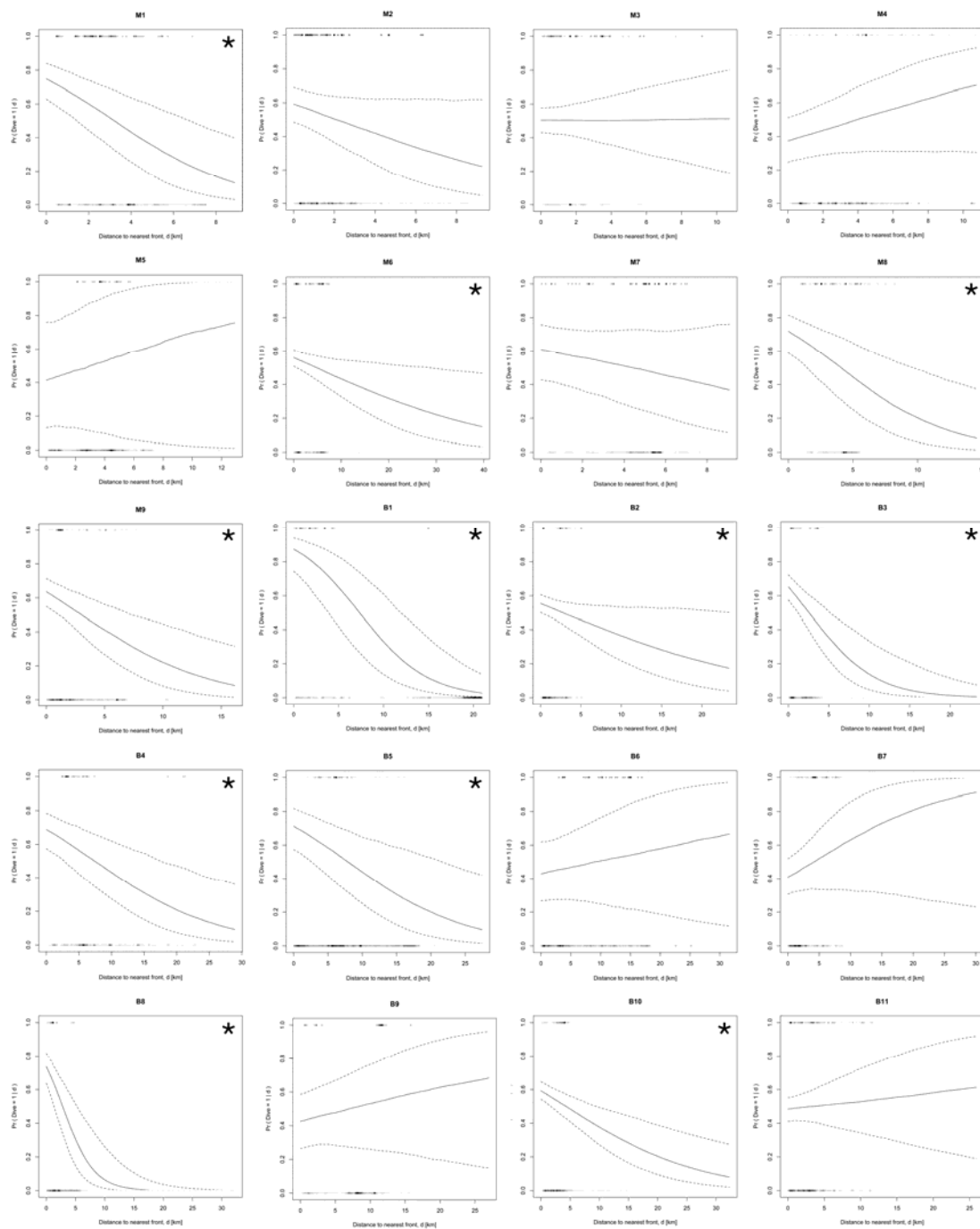
20 Section 3. ARS activity vs. fronts



21

22 Figure S3. (a-t) Behavioral shift depending on the distance to fronts in all tracks
 23 investigated. Fractal dimension D computed along the track is given as a function of
 24 the distance to the fronts d . The shift d_{shift} is indicated by the vertical dotted line. The
 25 mean and 95% confidence interval are represented by the solid and dashed lines
 26 (respectively) for the subset $\leq d_{shift}$ and $> d_{shift}$.

27 Section 4. Diving activity vs. fronts



28

29 Figure S4. (a-t) Probability of diving as a function of distance to fronts in the 20
 30 tracks investigated. The range of distances varies. Solid lines represent the mean
 31 effect and dashed lines represent 95% confidence. The density of observations of
 32 diving activity is given at $Pr(Dive = 1)$ and $Pr(Dive = 0)$ (grey shading). “*”
 33 indicates that the effect of d is significant.